The Nanoindentation Characteristics of Cu_6Sn_5, Cu_3Sn, and Ni_3Sn_4 Intermetallic Compounds in the Solder Bump

GUH-YAW JANG,[1] JYH-WEI LEE,[2] and JENQ-GONG DUH[1,3]

1.—Department of Materials Science and Engineering, National Tsing Hua University, Hsinchu 300, Taiwan. 2.—Department of Mechanical Engineering, Tung Nan Institute of Technology, Taipei 222, Taiwan. 3.—E-mail: jgd@mx.nthu.edu.tw

In general, formation and growth of intermetallic compounds (IMCs) play a major role in the reliability of the solder joint in electronics packaging and assembly. The formation of Cu-Sn or Ni-Sn IMCs have been observed at the interface of Sn-rich solders reacted with Cu or Ni substrates. In this study, a nanoindentation technique was employed to investigate nanohardness and reduced elastic moduli of Cu_6Sn_5, Cu_3Sn, and Ni_3Sn_4 IMCs in the solder joints. The Sn-3.5Ag and Sn-37Pb solder pastes were placed on a Cu/Ti/Si substrate and Ni foil then annealed at 240°C to fabricate solder joints. In Sn-3.5Ag joints, the magnitude of the hardness of the IMCs was in the order $Ni_3Sn_4 > Cu_6Sn_5 > Cu_3Sn$, and the elastic moduli of Cu_6Sn_5, Cu_3Sn, and Ni_3Sn_4 were 125 GPa, 136 GPa, and 142 GPa, respectively. In addition, the elastic modulus of the Cu_6Sn_5 IMC in the Sn-37Pb joint was similar to that for the bulk Cu_6Sn_5 specimen but less than that in the Sn-3.5Ag joint. This might be attributed to the strengthening effect of the dissolved Ag atoms in the Cu_6Sn_5 IMC to enhance the elastic modulus in the Sn-3.5Ag/Cu joint.

Key words: Sn-Ag solder, intermetallic compound (IMC), hardness, elastic modulus

INTRODUCTION

Flip-chip technology provides many beneficial advantages, including high reliability, high input/output connections, and low cost assembly.[1,2] Silicon chips with solder bumps are placed face to connect with a metallized substrate. An under-bump metallization (UBM) is used to provide adhesion and act as a diffusion barrier between solders and Si chips. Available UBM structures include Cu/Cr/Cr, Cu/Cu/Ti, Cu/Ni(V)/Al, and Ni/Cu/Ti.[3–5] After soldering, the growth of 1–2 μm of an intermetallic compound (IMC) formed between the solder and UBM is considered an indicator of good metallurgical bond and wetting.[6] However, IMCs have been a major reliability concern after multiple reflows and lengthy aging, resulting in the excessive growth of existing compounds, such as Cu_6Sn_5, or the formation of another compound in the edge of the solder bump, such as Cu_3Sn.[7–9] Strength and lifetime of solder joints might be decreased because of fracture through the IMCs.

The Sn-Pb solder alloys are widely used in today's electronic package. However, because of the toxic effect of Pb on humans and the environment, the microelectronics industry faces a global environmental demand for increased usage of Pb-free solders.[10,11] The Sn-3.5Ag solder alloy with a eutectic point of 221°C is considered one of the candidates because of its better mechanical properties.[12]

In the literature, the hardness and elastic modulus of bulk Cu-Sn and Ni-Sn IMCs was reported; however, there exists appreciable disagreement for the values of elastic modulus and hardness for IMCs.[13–15] The data concerning the hardness and elastic modulus of Cu-Sn IMCs in the solder joint is limited.[16,17] Furthermore, up to today, there is few literature data concerning the hardness and elastic modulus of the Ni-Sn IMC in the solder joint. It is thus interesting to evaluate the hardness and elastic modulus of Cu_6Sn_5, Cu_3Sn, and Ni_3Sn_4 IMCs in Sn-3.5Ag and Sn-37Pb solder joints. In this study, two kinds of

(Received March 13, 2004; accepted April 29, 2004)

substrate, i.e., Cu/Ti/Si and Ni foil, were used. In addition, the effect of Ag atoms dissolved in the Cu_6Sn_5 IMC on the hardness and elastic modulus was also discussed in the Sn-3.5Ag/Cu/Ti/Si joint.

EXPERIMENTAL PROCEDURES

Two different compositions of solder paste materials were used in the present study. One was the lead-free Sn-3.5Ag solder and the other was the eutectic Sn-37Pb solder. The solder paste was placed on the Cu/Ti/Si substrate and Ni foil, respectively, and then annealed at 240°C. Annealing times were chosen such that an IMC with a thickness of 5 μm could be grown in the solder joints. For the Cu/Ti/Si substrate, the adhesion layer was sputtered Ti of 1,000 Å on the Si wafer. For the electroplated seed layer, 5,000-Å Cu was then sputtered on Ti. The electroplated Cu with 5-μm thickness was further deposited on the metallized substrate. In addition, the thickness and purity of the Ni foil were 0.125 mm and 99.9%.

These solder joints were cold-mounted in epoxy, sectioned by using a slow-speed diamond saw, and ground and polished for cross-sectional analysis. The morphologies of interfacial products between solders and UBM were analyzed with field-emission scanning electron microscopy (FE-SEM, JSM-6500F, JEOL, Japan Electron Optics Laboratory, Tokyo). The compositions of phases in the solder joints and elemental distribution across the joint interface were quantitatively measured with an electron probe microanalyzer (EPMA, JXA-8800M, JEOL) with the aid of a ZAF (Z = atomic number factor, A = absorption factor, F = characteristic fluorescence) program.[18]

Two ingots of Cu_6Sn_5 and Cu_3Sn IMCs were also tested in this study. These IMCs were prepared from pure metals (higher than 99.9% purity). Samples were encapsulated in quartz tubes under vacuum, melted, and held at 1,150°C for 1 week. The quartz tubes were shaken every 12 h for homogenization during melting. All samples were polished and tested in the same manner for both Sn-3.5Ag and Sn-37Pb solder joints.

The nanoindentation test for the IMCs in both solder joints and bulk samples was investigated by means of a nanoindenter (TriboScope, Hysitron, Minneapolis, MN) interfaced with atomic force microscopy (AFM, Nanoscope E, Digital Instrument, Santa Barbara, CA). The nanoindenter was equipped with a Berkovich 142.3° diamond-probe tip, three-sided pyramidal indenter. The tip radius is around 100 nm. The cross-sectional morphologies of solder joints were inspected with AFM first. After the area of interest was focused, the nanoindentation test was conducted under 1,000 μN loads. The loading and unloading rates of the nanoindentation were all 200 μN/sec. The holding time was 5 sec. The AFM impressions of indents were observed with the identical indentation-diamond tip. The nanohardness and reduced elastic modulus of each indent was determined on the basis of the Oliver and Pharr method.[19] The reduced elastic modulus, E_r, was expressed as

$$E_r = \left(\frac{1-\nu^2}{E} + \frac{1-\nu_i^2}{E_i} \right)^{-1} \quad (1)$$

where E and ν are the elastic modulus and Poisson's ratio, respectively, for the specimen under test, and E_i (1,140 GPa) and ν_i (0.07) are the corresponding parameters of the diamond indenter.

RESULTS AND DISCUSSION

Interfacial Reaction in Solder/Cu and Solder/Ni Joints

The Sn-3.5Ag/Cu and Sn-37Pb/Cu joints were annealed at 240°C for 1 h, 2 h, and 3 h. In the case of Sn-3.5Ag/Cu joints annealed at 240°C for 1 h and 2 h, there were two types of reaction product formed between the Sn-3.5Ag solder and the Cu substrate. One was the layered reaction product above the Cu layer and the other was scallop-like between the solder and the layered reaction product. The morphology of the Sn-3.5Ag/Cu joint annealed for 1 h looks similar to that annealed for 2 h. However, the Cu metallization was consumed completely in the Sn-3.5Ag/Cu joint after 3 h of annealing. Thus, only the result for the Sn-3.5Ag solder joint annealed at 240°C for 2 h is typically presented in Fig. 1a. The size of the layered reaction product is around 1 μm and close to the detection limit of EPMA if the resolution of the electron probe size is considered. To obtain more reliable quantitative data, a deliberative task was carried out in the EPMA by selecting the appropriate accelerating voltage, beam current, and focus-beam size. It should be pointed out that the reported composition as listed in this study was the average of at least ten measured points. In the case of the Sn-3.5Ag/Cu joint annealed for 2 h, the composition of the scallop-type reaction product was 44.75at.%Sn, 55.01at.%Cu, and 0.24at.%Ag, as shown in Table I. Therefore, this reaction product could be denoted as the Cu_6Sn_5 IMC. On the other hand, the composition of the layered-type reaction product was 24.5at.%Sn, 75.4at.%Cu, and 0.10at.%Ag after quantitative analysis by EPMA, and this product was identified as the Cu_3Sn IMC. It is clearly demonstrated from the composition of the Cu_6Sn_5 and Cu_3Sn IMCs by EPMA that a few Ag atoms were dissolved from the Sn-3.5Ag solder into the Cu_6Sn_5 and Cu_3Sn IMCs. To investigate the detailed variation of the composition of Ag in Cu_6Sn_5 and Cu_3Sn IMCs, an electron microprobe trace was drawn across the interface of the Sn-3.5Ag/Cu joint annealed at 240°C after 2 h, as shown in Fig. 2. It is indicated in Fig. 2b that Ag concentrations in the Cu_6Sn_5 and Cu_3Sn IMCs are maintained around 0.24 at.% and 0.1 at.%, respectively.

Two reaction products formed between the Sn-37Pb solder and Cu metallization in the Sn-37Pb/Cu joint annealed at 240°C for 1 h, 2 h, and 3 h. The cross-sectional morphologies of the Sn-37Pb/Cu joints annealed for 1 h and 2 h was similar to that annealed

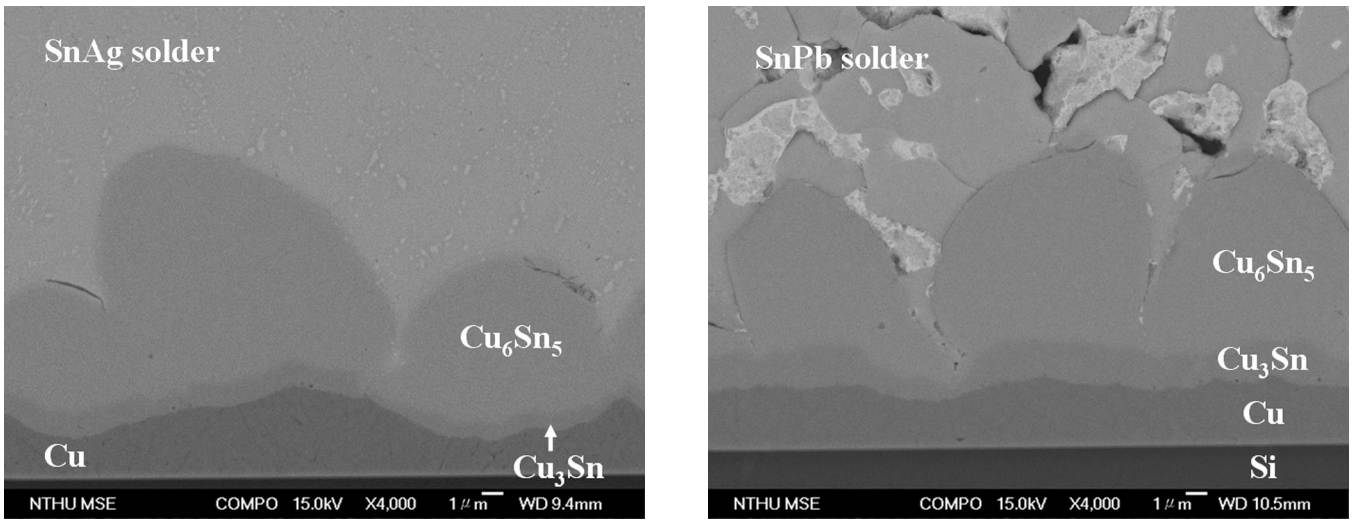

a b

Fig. 1. Cross-sectional images of interfacial morphology in the solder/Cu joint annealed at 240°C: (a) Sn-3.5Ag for 2 h and (b) Sn-37Pb solder for 3 h.

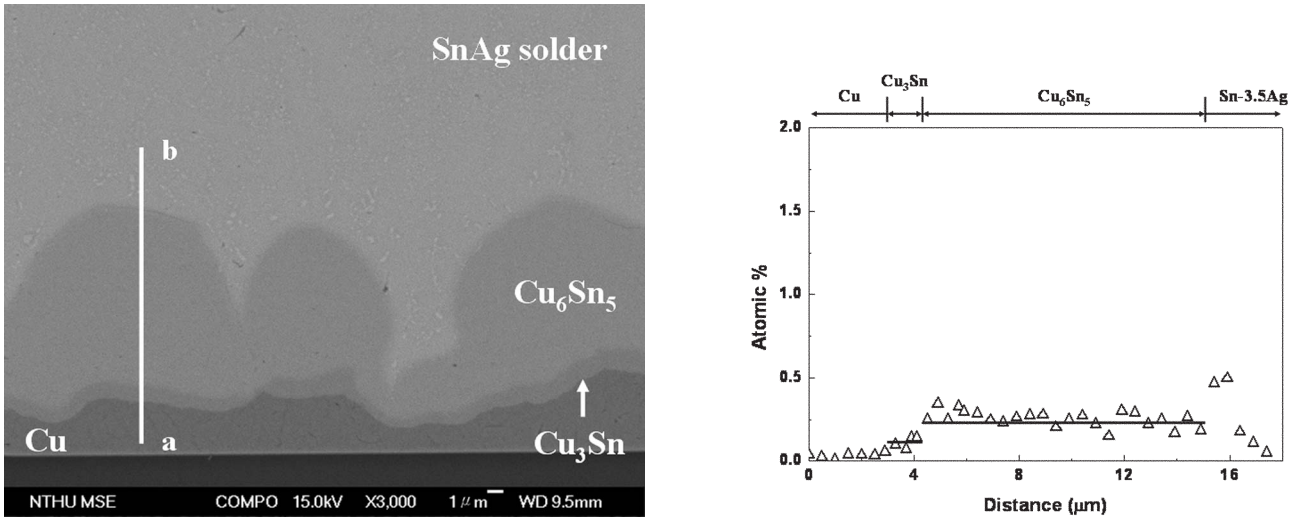

a b

Fig. 2. (a) Cross-sectional image of Sn-3.5Ag solder/Cu interface in the joint annealed at 240°C for 2 h and (b) the concentration profile of Ag along trace line ab.

for 3 h (Fig. 1b). The composition of the scalloped-type reaction product was 44.77at.%Sn and 55.23at.%Cu in the Sn-37Pb/Cu joint annealed for 3 h (Table I). Therefore, the scalloped-type product could be considered the Cu_6Sn_5 IMC. With the aid of the quantitative analysis of EPMA, the layered-type reaction product was identified as Cu_3Sn. In addition, the thickness of the Cu_6Sn_5 IMC was greater than 8 μm in both the Sn-3.5Ag/Cu joint annealed for 2 h and the Sn-37Pb/Cu joint annealed for 3 h. Thus, the size of the Cu_6Sn_5 and Cu_3Sn IMCs in these joints was sufficient to be analyzed for nanoindentation test.

Only the scalloped-type reaction product formed between the solder and the Ni layer in both Sn-3.5Ag/Ni

Table I. Composition of IMCs Formed in Various Solder Joints

Specimen	IMC Type	IMC Composition (at.%)
SnAg/Cu joint annealed for 2 h	Cu_6Sn_5	44.75 ± 0.51 Sn, 55.01 ± 0.51 Cu, 0.24 ± 0.03 Ag
	Cu_3Sn	24.50 ± 0.38 Sn, 75.40 ± 0.37 Cu, 0.10 ± 0.03 Ag
SnPb/Cu joint annealed for 3 h	Cu_6Sn_5	44.77 ± 0.44 Sn, 55.23 ± 0.44 Cu
	Cu_3Sn	24.12 ± 0.30 Sn, 75.88 ± 0.30 Cu
SnAg/Ni joint annealed for 24 h	Ni_3Sn_4	57.76 ± 0.42 Sn, 43.24 ± 0.42 Ni
SnPb/Ni joint annealed for 24 h	Ni_3Sn_4	57.21 ± 0.49 Sn, 42.79 ± 0.49 Ni

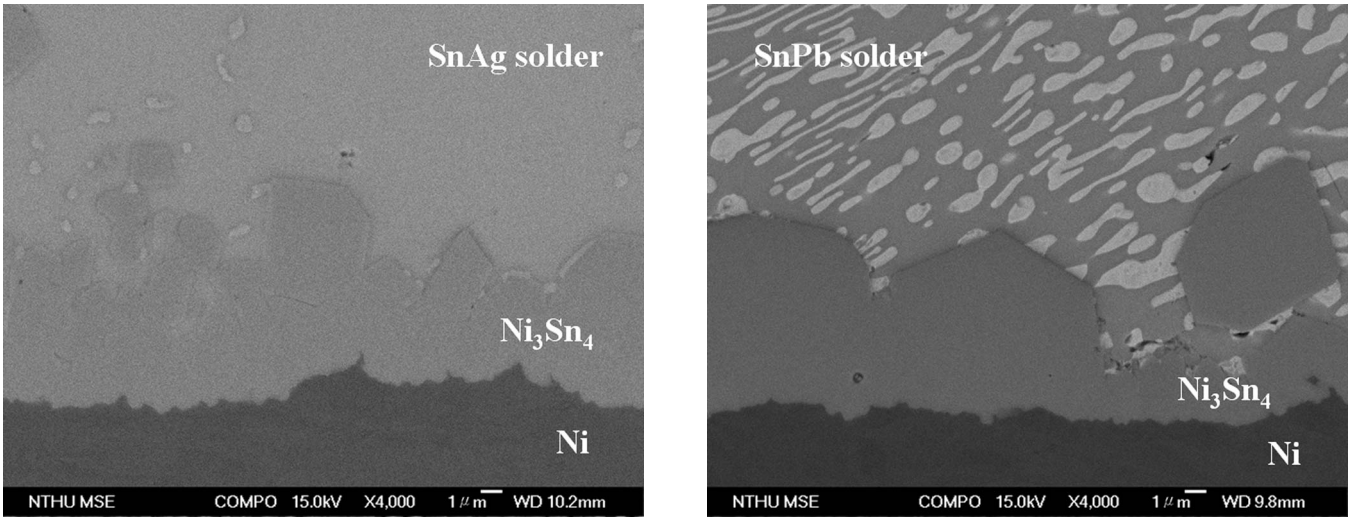

a b

Fig. 3. Cross-sectional images of interfacial morphology in the solder/Ni joint annealed at 240°C for 24 h: (a) Sn-3.5Ag and (b) Sn-37Pb solders.

and Sn-37Pb/Ni joints annealed at 240°C for 5 h, 12 h, and 24 h. After quantitative analysis of EPMA, the ratio of Ni:Sn for the scalloped-type reaction product was 3:4 (Table I). Thus, it should be considered the Ni_3Sn_4 IMC. Figure 3 shows the interfacial morphology of Sn-3.5Ag/Ni and Sn-37Pb/Ni joints annealed for 24 h. It is clearly indicated that the thickness of the Ni_3Sn_4 IMC in Sn-3.5Ag/Ni and Sn-37Pb/Ni was 6.33 ± 1.7 μm and 6.13 ± 2.31 μm, respectively. Thus, the solder/Ni joints annealed at 240°C for 24 h sufficed to be analyzed by nanoindentation test.

Nanoindentation Test

Figure 4 shows the AFM images of interfacial morphology in Sn-3.5Ag/Cu and Sn-3.5Ag/Ni joints annealed at 240°C for 2 h and 24 h, respectively. The interfaces among the Sn-3.5Ag solder, Cu_6Sn_5, Cu, and Si in the Sn-3.5Ag/Cu joint are clearly observed by AFM (Fig. 4a). Similarly, the AFM image (Fig. 4b) obviously displays the Sn-3.5Ag solder/Ni_3Sn_4 and Ni_3Sn_4/Ni interfaces in the Sn-3.5Ag/Ni joint. Thus, the indentation test can be carried out within any desired phase in the solder joints with AFM images except for the Cu_3Sn IMC. In addition, it should be pointed out that reported hardness and reduced elastic modulus as listed in this study were the average of at least 15 measured points.

Nanoindentation Test for Solder/Cu Joints

The AFM image clearly exhibits the interface between the Cu-Sn IMC and Cu metallization in

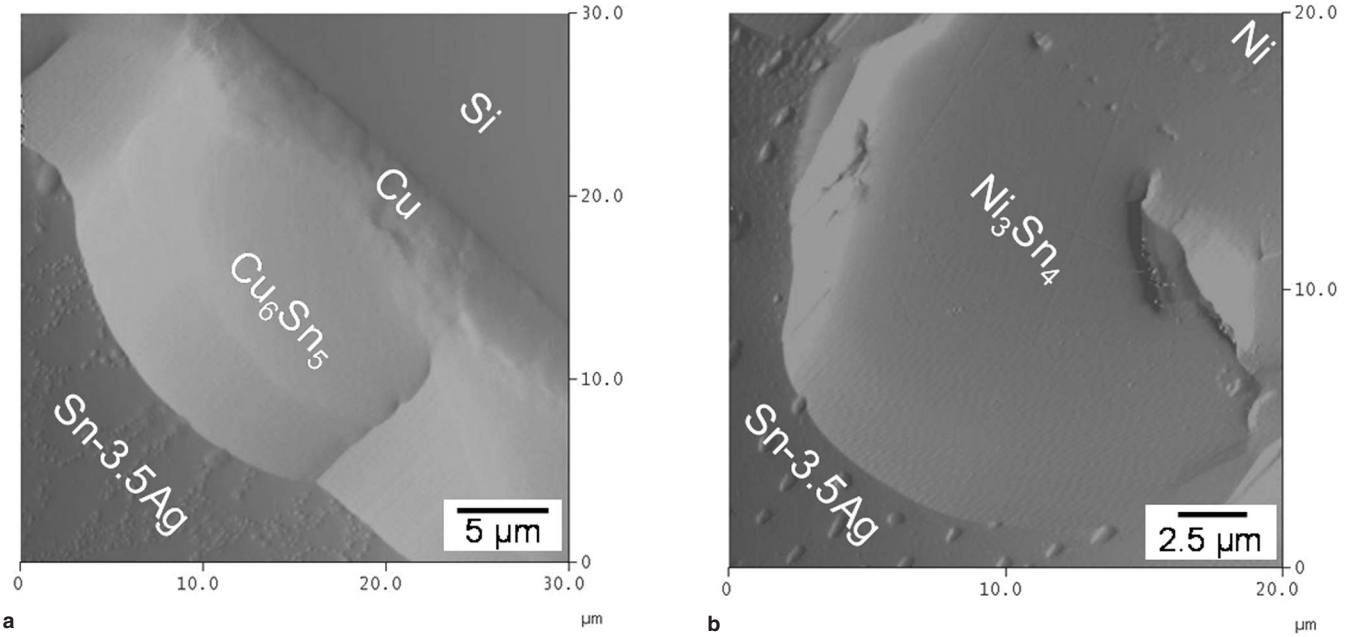

a b

Fig. 4. The AFM images of interfacial morphology in the (a) Sn-3.5Ag/Cu joint annealed for 2 h and (b) Sn-3.5Ag/Ni joint annealed for 24 h.

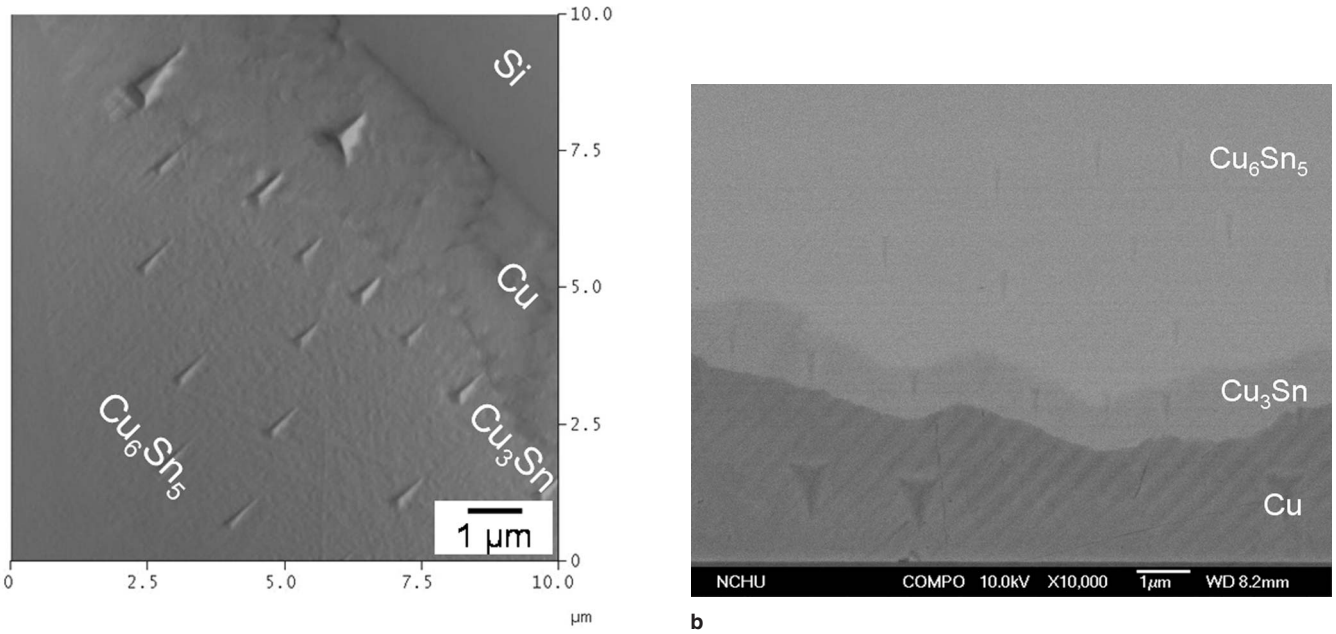

Fig. 5. (a) The AFM and (b) BEI images for the indents in the Cu_6Sn_5, Cu_3Sn, and Cu for the Sn-3.5Ag/Cu joint annealed at 240°C for 2 h.

the Sn-3.5Ag/Cu joint. However, the Cu_6Sn_5/Cu_3Sn interface was not so visible, as displayed in Fig. 5a. It is also indicated from Fig. 1a that the thickness of Cu_3Sn was maintained around 1 μm in the Sn-3.5Ag/Cu joint annealed at 240°C for 2 h. Combining the backscattered electron image (BEI) of the interfacial morphology in the Sn-3.5Ag/Cu joint, the position of the Cu_3Sn IMC in the AFM image could be located. After nanoindentation test, the locations of indents were re-confirmed by FE-SEM (Fig. 5b).

The load-depth curves collected for indents performed in various phases for the Sn-3.5Ag/Cu joint annealed for 2 h exhibit different shapes because of the large differences in hardness between the materials. Indents performed in the Sn-3.5Ag solder, Cu_6Sn_5, and within Cu are shown in Fig. 6a. The hardness calculated for each of these tests is 0.5 GPa (Sn-3.5Ag solder), 6.1 GPa (Cu_6Sn_5), and 2.16 GPa (Cu). Besides, the hardness difference examined between indents in the Cu_6Sn_5 and Cu_3Sn IMCs was rather small (Fig. 6b). The hardness of the Cu_3Sn IMC was 5.69 GPa, quite similar to that of the Cu_6Sn_5 IMC. On the other hand, the reduced elastic modulus calculated from this test for the Sn-3.5Ag solder, Cu_6Sn_5, Cu_3Sn, and Cu is 51.6 GPa, 123 GPa, 132 GPa, and 111 GPa, respectively, in the Sn-3.5Ag/Cu joint annealed for 2 h, as shown in Table II. In addition, it was found in examining the shape of the residual indents that none of Cu_6Sn_5, Cu_3Sn IMCs, and pure Cu exhibited pileup behavior (Fig. 5a). On the other hand, Fig. 7 displays the shape of the residual indent for the SnAg solder. It is evident that the SnAg solder reveals pileup behavior.

A nanoindentation test was performed in the Sn-37Pb/Cu joint annealed at 240°C for 3 h. Figure 8 is a plot of load depth for indentations performed in Cu_6Sn_5 IMCs in both Sn-3.5Ag/Cu and Sn-37Pb/

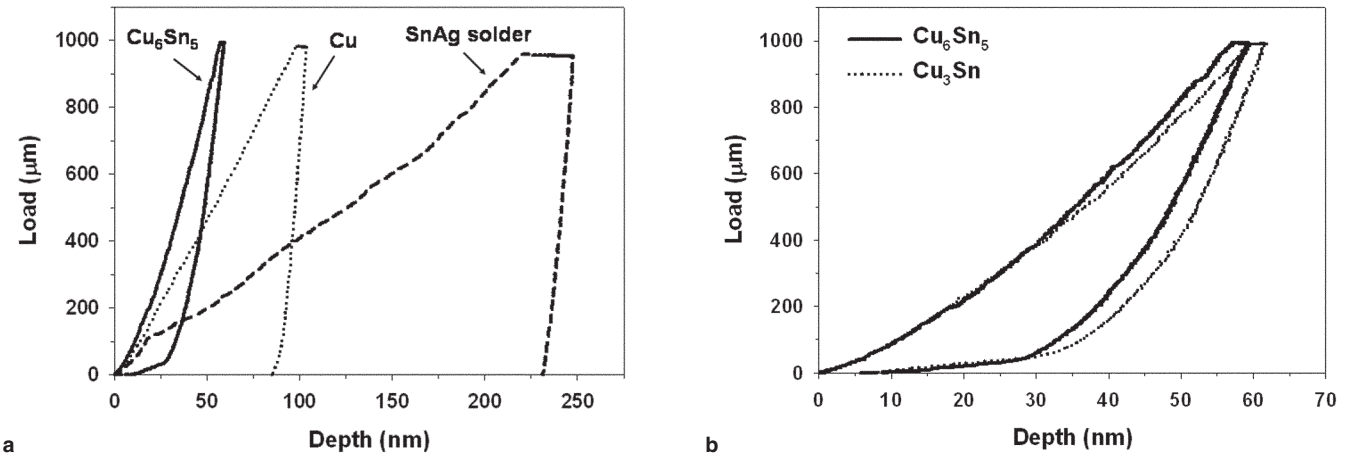

Fig. 6. The load-depth curves for (a) the Cu_6Sn_5 IMC (solid line), Cu (dotted line), and SnAg solder (dashed line); and (b) the Cu_3Sn IMC (dotted line) in the Sn-3.5Ag/Cu joint annealed at 240°C for 2 h.

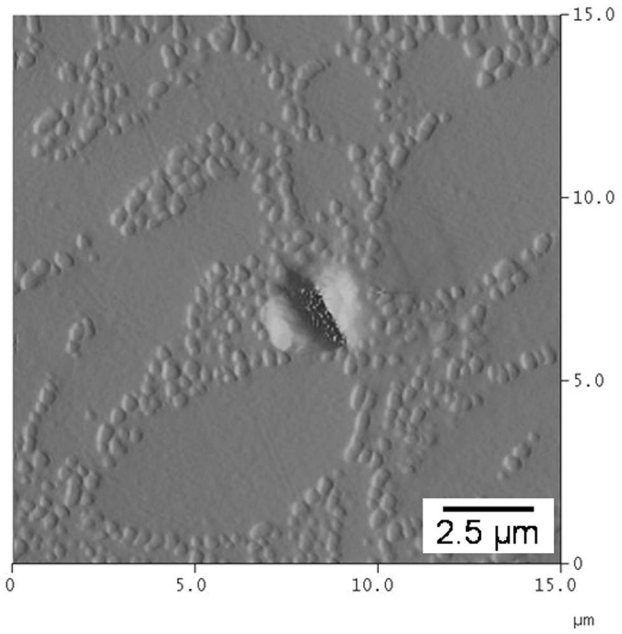

Fig. 7. The AFM images of morphologies of indents in the SnAg solder for the Sn-3.5Ag/Cu joint annealed at 240°C for 2 h.

Cu joints. It is evident in Table II that the hardness of the Cu_6Sn_5 IMC in the Sn-37Pb/Cu joint, i.e., 5.62 GPa, was smaller than that in the Sn-3.5Ag/Cu joints. The reduced elastic modulus of the Cu_6Sn_5 IMC in the Sn-37Pb/Cu joint was 115.6 ± 3.5 GPa, less than that of the Cu_6Sn_5 IMC in the Sn-3.5Ag system. As mentioned previously, the Cu_6Sn_5 IMC in the Sn-3.5Ag/Cu joint dissolved Ag atoms during annealing (Fig. 2). It is argued that the hardness and reduced elastic modulus of the Cu_6Sn_5 IMC in the Sn-3.5Ag/Cu joint might be enhanced by the dissolved Ag atoms.

In the case of the bulk Cu_6Sn_5 and Cu_3Sn sample, AFM imaging was less critical for ensuring that the proper phase was tested, primarily, because of the larger area available for the phases of interest. Table II shows the hardness and reduced elastic modulus measured in this bulk Cu_6Sn_5 and Cu_3Sn specimens. The hardnesses of bulk Cu_6Sn_5 and

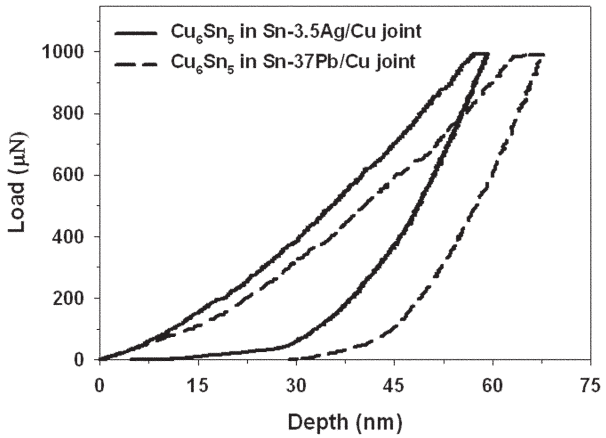

Fig. 8. Load-depth curves for the Cu_6Sn_5 IMC in the Sn-3.5Ag/Cu joint annealed for 2 h (solid line) and in the Sn-37Pb/Cu joint annealed for 3 h (dashed line).

Cu_3Sn were 6.27 GPa and 5.72 GPa, quite similar to that in the Sn-3.5Ag/Cu joint. Combining data from bulk Cu-Sn IMCs and the Sn-3.5Ag/Cu joint, it is clearly indicated that the hardness of the Cu_6Sn_5 IMC was greater than that of the Cu_3Sn IMC, while the reduced elastic modulus showed the reverse.

Nanoindentation Test for Solder/Ni Joints

Figure 9 shows the residual indents in the Ni and Ni_3Sn_4 IMC for the Sn-3.5Ag/Ni joint annealed at 240°C for 24 h. In examining the shape of the residual indents, it was found that there was no pileup phenomenon for the Ni_3Sn_4 IMC; however, the Ni displayed pileup. Figure 10 exhibited the load-depth curves of the Ni_3Sn_4 IMC in the Sn-3.5Ag/Ni joint as well as Cu-Sn IMCs in the Sn-3.5Ag/Cu joint. It is evident from the nanoindentation data that Ni_3Sn_4 is significantly harder than Cu_6Sn_5 and Cu_3Sn IMCs, for the hardness calculated from the curve of Fig. 10 was as high as 8.09 GPa. In addition, the reduced elastic modulus of Ni_3Sn_4 and Ni in the Sn-3.5Ag/Ni joint was 140.4 ± 7.9 and 157.4 ± 3.8, respectively (Table II). In fact, the hardness and reduced elastic modulus of Ni_3Sn_4 in the Sn-37Pb/Ni joint was quite similar to that in the Sn-3.5Ag/Ni joint.

Table II. Hardness and Reduced Elastic Modulus (Er) for the SnAg Solder, Cu_6Sn_5, Cu_3Sn, Ni_3Sn_4, Cu, and Ni in the Solder Joints and Bulk Specimens

Material	Specimen	Hardness (GPa)	Er (GPa)
SnAg solder	Sn-3.5Ag/Cu joint	0.50 ± 0.07	51.7 ± 2.7
Cu_6Sn_5	Sn-3.5Ag/Cu joint	6.10 ± 0.53	123.3 ± 6.0
	Sn-37Pb/Cu joint	5.62 ± 0.35	115.6 ± 3.5
	Bulk	6.27 ± 0.30	114.4 ± 1.3
Cu_3Sn	Sn-3.5Ag/Cu joint	5.69 ± 0.58	131.9 ± 5.0
	Bulk	5.72 ± 0.34	119.7 ± 5.5
Ni_3Sn_4	Sn-3.5Ag/Ni joint	8.12 ± 0.62	140.4 ± 7.9
	Sn-37Pb/Ni joint	8.90 ± 0.55	136.4 ± 6.0
Cu	Sn-3.5Ag/Cu joint	2.16 ± 0.19	110.8 ± 3.8
	Sn-37Pb/Cu joint	2.08 ± 0.17	112.3 ± 3.3
Ni	Sn-3.5Ag/Ni joint	3.69 ± 0.25	157.4 ± 3.8
	Sn-37Pb/Ni joint	3.63 ± 0.33	154.6 ± 4.6

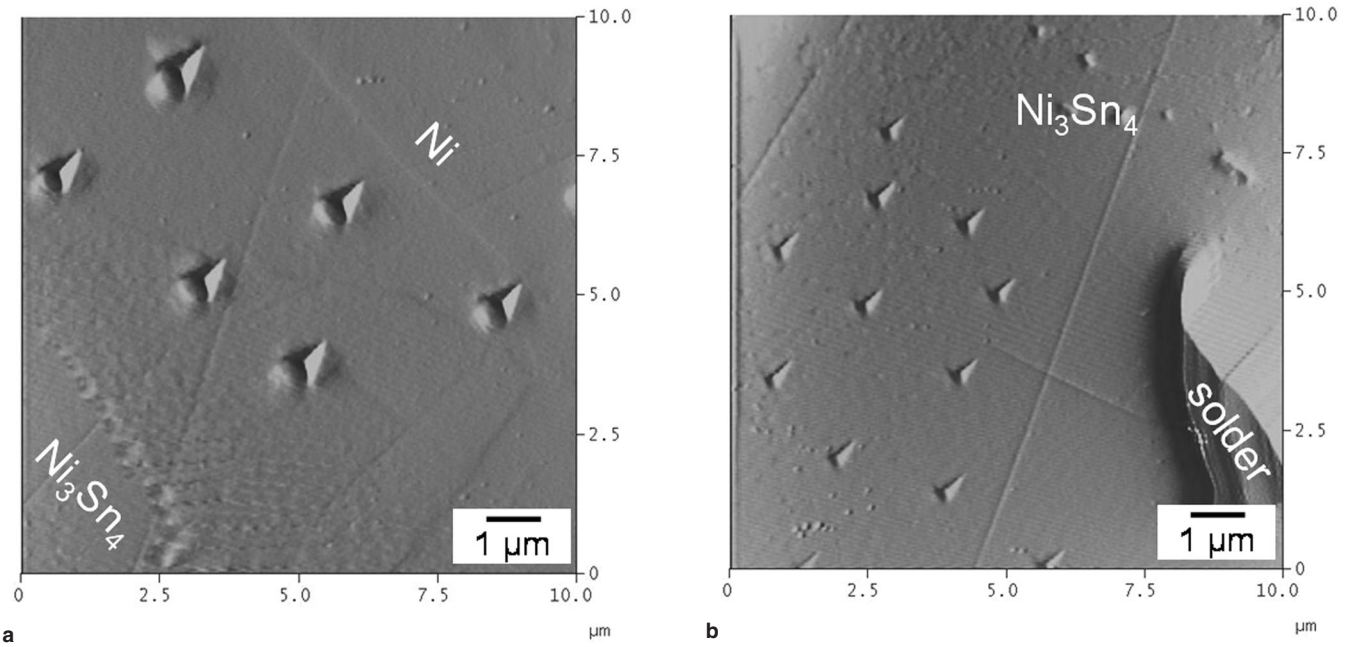

Fig. 9. The AFM images of morphologies for indents in (a) Ni and (b) the Ni_3Sn_4 IMC for the Sn-3.5Ag/Ni joint annealed at 240°C for 24 h.

Comparisons of Hardness and Elastic Modulus

The reduced elastic moduli of Cu_6Sn_5, Cu_3Sn, and Ni_3Sn_4 IMCs have been measured in this study. In the literature, Fields et al.[14] reported that the Poisson's ratio of Cu_6Sn_5, Cu_3Sn, and Ni_3Sn_4 IMCs were 0.309, 0.299, and 0.330, respectively. To compare with data in the literature, the elastic moduli of Cu_6Sn_5, Cu_3Sn, and Ni_3Sn_4 IMCs can be calculated with the Poisson's ratio measured by Fields et al.[14] Table III shows hardness and elastic modulus for Cu_6Sn_5, Cu_3Sn, and Ni_3Sn_4 IMCs as determined in this study and by other investigators.[13–17] Chromik et al. reported that the hardness of the Cu_6Sn_5 IMC decreased with increasing indenter penetration, which was attributed to the indentation size effect.[17] In studies of Kang et al.[13] and Fields et al.,[14] the hardness of Cu_6Sn_5, Cu_3Sn, and Ni_3Sn_4 IMCs was measured by microindentation with a Vickers indenter; thus, the indenter penetration in their studies was greater than that in this study. As a result, the hardness of these IMCs measured by Kang et al. and Fields et al. was less than that in this study. Nevertheless, the indenter penetration in the Cu-Sn IMC in the study was similar to that reported by Chromik et al.[17] It is apparent in all studies that the hardness of the Cu_6Sn_5 IMC was greater than that of the Cu_3Sn IMC. In addition, the work by Fields et al. exhibited the only other measurement for hardness of the Ni_3Sn_4 IMC,[14] in which the hardness of the Ni_3Sn_4 IMC was between Cu_6Sn_5 and Cu_3Sn IMCs. However, the evaluated hardness of the Ni_3Sn_4 IMC was greater than Cu_6Sn_5 and Cu_3Sn IMC in this study.

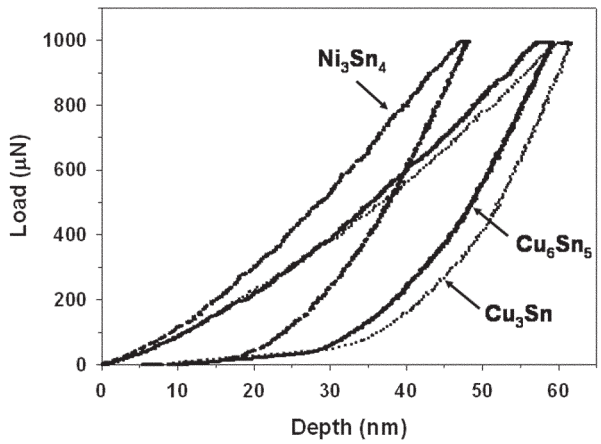

Fig. 10. Load-depth curves for the Ni_3Sn_4 (dashed line) IMC in the Sn-3.5Ag/Ni joint annealed for 24 h and also for Cu_6Sn_5 (solid line) and Cu_3Sn (dotted line) IMCs in the Sn-3.5Ag/Cu joint annealed for 2 h.

In the works of Chromik et al.[17] and Ostrovskaya,[15] the elastic modulus of the Cu_6Sn_5 IMC was less than that of the Cu_3Sn IMC. This is consistent with data in the Sn-3.5Ag solder joint and bulk specimen in this study. In the literature, Fields et al. were the only ones to report the elastic modulus of the Ni_3Sn_4 IMC.[14] The magnitude of elastic modulus in these IMCs was $Ni_3Sn_4 > Cu_3Sn > Cu_6Sn_5$. This trend was identical with that in the Sn-3.5Ag solder joint in this study. Furthermore, the elastic modulus of the Cu_6Sn_5 IMC in the Sn-37Pb joint was similar to that for the bulk specimen but less than that in the Sn-3.5Ag joint (Table III). This is due to the dissolved Ag atoms that enhanced the elastic modulus of the Cu_6Sn_5 IMC in the Sn-3.5Ag/Cu joint, as previously mentioned.

CONCLUSIONS

The Cu_6Sn_5 and Cu_3Sn IMCs formed in the solder/Cu joint annealed at 240°C. During annealing, Ag atoms dissolved into Cu_6Sn_5 and Cu_3Sn IMCs in

Table III. Collected Data for Hardness and Elastic Modulus of Cu_6Sn_5, Cu_3Sn, and Ni_3Sn_4 IMCs

Sample Description	Experimental Technique	Cu_6Sn_5		Cu_3Sn		Ni_3Sn_4		Remarks
		Hardness (GPa)	E (GPa)	Hardness (GPa)	E (GPa)	Hardness (GPa)	E (GPa)	
Sn-3.5Ag joint annealed at 240°C	Nanoindentation (Berkovich)	6.10 ± 0.53	125 ± 6.8	5.69 ± 0.58	135.7 ± 5.9	8.12 ± 0.62	142.7 ± 9.2	This study
Sn-37Pb/Cu joint annealed at 240°C	Nanoindentation (Berkovich)	5.62 ± 0.35	116.3 ± 3.9	—	—	8.9 ± 0.55	138 ± 7	This study
Bulk specimens, casting	Nanoindentation (Berkovich)	6.27 ± 0.30	114.9 ± 1.5	5.72 ± 0.34	121.7 ± 6.2	—	—	This study
Cu/Sn diffusion couples	Microindentation (Vickers)	4.41 ± 0.21	—	4.22 ± 0.15	—	—	—	Kang et al.[13]
Bulk specimens, hot isostatic press	Microindentation (Vickers)	3.71 ± 0.54	85.6 ± 1.7	3.36 ± 0.46	108.3 ± 4.4	3.58 ± 0.07	133.3 ± 5.6	Fields et al.[14]
Solid-state aging of diffusion couple	Nanoindentation (Berkovich)	6.5 ± 0.3	119 ± 6	6.2 ± 0.4	143 ± 7	—	—	Chromik et al.[16,17]
Thick films, vacuum deposition	Resonance	—	102	—	153	—	—	Ostrovskaya et al.[15]

the Sn-3.5Ag/Cu joint. In addition, the Ni_3Sn_4 IMC formed in the solder/Ni annealed at 240°C.

The magnitude of hardness measured by nanoindentation was in the order $Ni_3Sn_4 > Cu_6Sn_5 > Cu_3Sn$. The elastic modulus of Cu_6Sn_5, Cu_3Sn, and Ni_3Sn_4 IMCs in Sn-3.5Ag joints was 125 GPa, 136 GPa, and 143 GPa, respectively.

The elastic modulus of the Cu_6Sn_5 IMC in the Sn-37Pb joint was similar to that for the bulk specimen but less than that in the Sn-3.5Ag joint. This might be attributed to the dissolved Ag atoms in the IMC that enhance the elastic modulus of the Cu_6Sn_5 IMC in the Sn-3.5Ag/Cu joint.

ACKNOWLEDGEMENTS

The financial support and joint assemblies preparation from Taiwan Semiconductor Manufacturing Company are acknowledged. Partial support from National Science Council under Contract No. NSC-92-2216-E007-037 is also appreciated.

REFERENCES

1. C.S. Chang, A. Oscilowski, and R.C. Bracken, *IEEE Circuit. Dev.* 14, 45 (1998).
2. J.H. Lau, *Flip Chip Technologies* (New York: McGraw-Hill, 1996), pp. 26–30.
3. K.L. Lin and Y.C. Liu, *Proc. Electronic Components Technology Conf.* (Piscataway, NJ: IEEE, 1999), pp. 607–612.
4. K. Zeng and K.N. Tu, *Mater. Sci. Eng. R* 38, 55 (2002).
5. C.S. Huang, J.G. Duh, Y.M. Chen, and J.H. Wang, *J. Electron. Mater.* 32, 89 (2003).
6. H.H. Manko, *Solders and Soldering* (New York: McGraw-Hill, 2001), pp. 61–167.
7. A.A. Liu, H.K. Kim, K.N. Tu, and P.A. Totta, *J. Appl. Phys.* 80, 2774 (1996).
8. H.K. Kim, K.N. Tu, and P.A. Totta, *Appl. Phys. Lett.* 68, 2204 (1996).
9. C.S. Huang, G.Y. Jang, and J.G. Duh, *J. Electron. Mater.* 32, 1273 (2003).
10. H.W. Miao and J.G. Duh, *Mater. Chem. Phys.* 71, 255 (2001).
11. D.R. Frear, J.W. Jang, J.K. Lin, and C. Zang, *JOM* 53, 28 (2001)
12. M. McCormack, S. Jin, G.W. Kammlott, and H.S. Chen, *Appl. Phys. Lett.* 63, 15 (1993).
13. J.S. Kang, R.A. Gagliano, G. Ghosh, and M.E. Fine, *J. Electron. Mater.* 31, 1238 (2002).
14. R.J. Fields, S.R. Low III, and G.K. Lucey, Jr. in *The Metal Science of Joining*, eds. M.J. Cieslak, J.H. Perepezko, S. Kang, and M.E. Glicksman (Warrendale, PA: TMS, 1991), pp. 165–174.
15. L.M. Ostrovskaya, V.N. Rodin, and A.I. Kuznetsov, *Sov. J. Non-Ferrous Metall. (Tsv. Metally)* 26, 90 (1985).
16. R.R. Chromik, R.P. Vinci, S.L. Allen, and M.R. Notis, *JOM* 55, 66 (2003).
17. R.R. Chromik, R.P. Vinci, S.L. Allen, and M.R. Notis, *J. Mater. Res.* 18, 2251 (2003).
18. J.I. Goldstein, *Scanning Electron Microscopy and X-ray Microanalysis* (New York: Plenum Press, 1992), pp. 306–330.
19. W.C. Oliver and G.M. Pharr, *J. Mater. Res.* 7, 1564 (1992).